Interactions of UHE cosmic ray nuclei with radiation during acceleration: consequences for the spectrum and composition

D. Allard* **and R.J. Protheroe†**

*Laboratoire Astroparticule et Cosmologie (APC)
Université Paris 7/CNRS, 10 rue A. Domon et L. Duquet, 75205 Paris Cedex 13, France.
†Department of Physics, School of Chemistry & Physics, The University of Adelaide, SA 5005, Australia.

***Abstract*. We study the diffusive shock acceleration of cosmic-ray protons and nuclei, taking into account all the relevant interaction processes with photon backgrounds. We investigate how the competition between protons and nuclei is modified by the acceleration parameters such as the acceleration rate, its rigidity dependence, the photon density and the confinement capability of the sources. We find that in the case of interaction-limited acceleration processes protons are likely to be accelerated to higher energies than nuclei, whereas for confinement-limited acceleration nuclei are accelerated to higher energies than protons. Finally, we discuss our results in the context of possible astrophysical accelerators, and in the light of recent cosmic-ray data.**

***Keywords*: acceleration, composition, ultra-high energy**

I. Interactions of nucleons and nuclei with radiation

We use the SOPHIA event generator for pion photoproduction (Mücke et al., [1]), continuous energy loss for Bethe-Heitler (BH) pair production [2] and the photon-nucleus interaction event generator developed by Allard et al. ([3], [4], [5], [6]) – see these papers for references to the original data compilations and fits. For the photon backgrounds in the infra-red, optical and ultra-violet window, we use a recent estimate [7] and re-scale its density with different scaling factors to account for the higher density IR/opt/UV backgrounds that could be expected in astrophysical sources. In Fig. 1 we show the energy dependence of the loss (or attenuation) length for cosmic-ray protons and Fe-nuclei in the CMB plus intergalactic IR/Opt/UV background (continuous line) and in the CMB plus an intergalactic IR/Opt/UV background 100 times higher (dashed line).

II. Diffusive shock acceleration

Diffusion of energetic particles in magnetic fields depends on their magnetic rigidity $\rho \equiv pc/Ze$ where p is the the particle's momentum and Ze its charge. In diffusive shock acceleration (DSA) the rigidity gain and escape rates depend on the diffusion coefficient which is usually assumed to have a power-law dependence on rigidity, $\kappa(\rho) \propto \rho^{\delta}$, with the exponent depending on the nature of the turbulence present in the magnetic field: $\delta = 1/3$ (Kolmogorov spectrum), 1/2 (Kraichnan spectrum) or 1 (completely disordered field). Detailed and rigorous treatments of DSA are given in several review articles (Drury [8], Blandford & Eichler [9], Berezhko & Krymsky [10], Jones & Ellison [11]).

In the absence of energy losses particles gain rigidity at an average rate $d\rho/dt = \rho r_{\rm gain}(\rho)$ while in the vicinity of the shock. The normalization of the gain rate $r_{\rm gain}(\rho)$ depends in a non-trivial way on the magnetic field, turbulence spectrum, shock configuration and shock velocity. We have therefore arbitrarily chosen to normalize the gain rate at a given cut-off rigidity to that necessary for protons to reach that given cut-off rigidity in a steady state situation, in the presence of the CMB and IR/Opt/UV radiation. The nominal cut-off rigidity for protons $\rho_{\rm cut}^{(p)}$ occurs where the gain rate equals the loss rate in the intergalactic IR/Opt/UV background,

$$r_{\rm gain}(\rho_{\rm cut}^{(p)}) = r_{\rm loss}(\rho_{\rm cut}^{(p)}, Z=1).$$

We have added to Fig. 1 curves representing $x_{\rm gain}(\rho) \equiv c/r_{\rm gain}(\rho) \propto \rho^{\delta}$ for different values of $\rho_{\rm cut}^{(p)}$ (assuming δ=1/3 and δ=1). We have chosen for $\rho_{cut}^{(p)}$ values in the range 10^{19} V to 10^{22} V. As the abscissa refers to the energy, and the acceleration depends on rigidity, the curves for the gain length for a given $\rho_{\rm cut}^{(p)}$ are shifted in energy proportionally to the charge (e.g. by a factor of 26 for Fe). Although the loss length is not strictly relevant for nuclei because nuclei do not remain on the same energy loss curve while losing energy, unlike protons, these figures show that the output of the acceleration process will crucially depend on the normalization of the background radiation and the gain rate and its rigidity dependence, and that the "competition" between protons and nuclei will, at least for some combinations of parameters, be non-trivial.

Box model approximation

In the box model of shock acceleration[12], [13], [14], [15], particles of magnetic rigidity ρ_0 are injected into the acceleration zone, or "box", and while inside the box are accelerated at a rate $r_{\rm tot}(\rho)$ and escape from the box at a rate $r_{\rm esc}(\rho)$. These two rates uniquely determine the spectrum of accelerated particles, i.e. those escaping from the box. The average rate of change of rigidity of a nucleus atomic number Z during shock acceleration

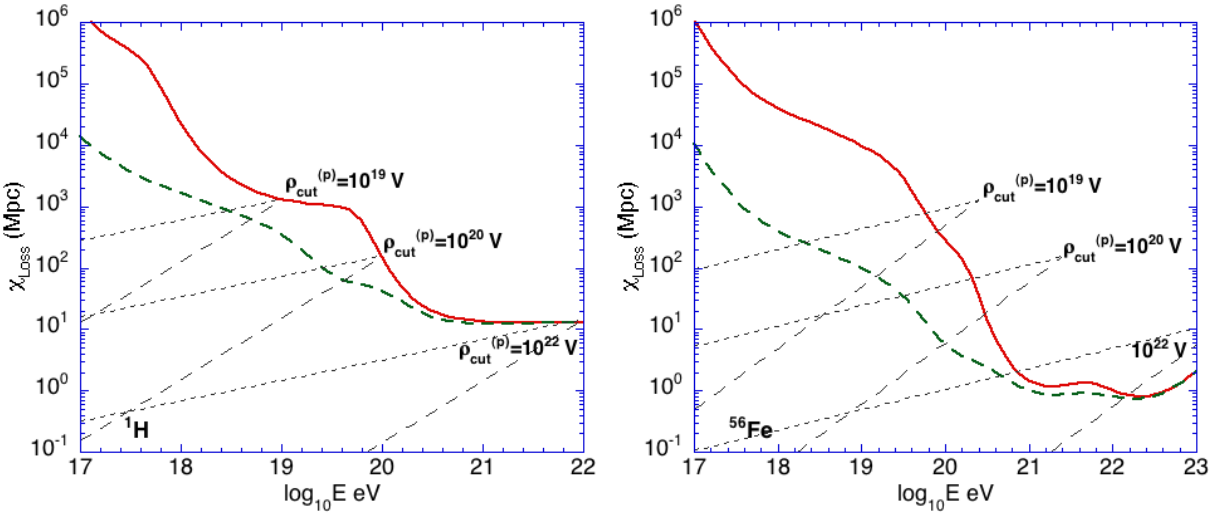

Fig. 1. Energy dependence of the loss length for cosmic-ray protons (left) and iron (right) in the CMB plus intergalactic IR/Opt/UV background (continuous line) and assuming a IR/Opt/UV background 100 times higher (dashed line). The loss length is compared to the gain length assuming three different values for $\rho_{cut}^{(p)}$ (10^{19}, 10^{20} and 10^{22} V) and $\delta = 1/3$ (thin short dashed lines) and $\delta = 1$ (thin long dashed lines).

with energy losses is

$$\left.\frac{d\rho}{dt}\right|_{\rm total,Z} \equiv \rho r_{\rm tot}(\rho, Z) = \rho\left[r_{\rm gain}(\rho) - r_{\rm loss}(\rho, Z)\right]$$

where $r_{\rm loss}(\rho, Z)$ includes both continuous energy losses and losses due to interactions. If there are no energy losses and no additional escape processes a power-law spectrum results, and the integral spectral index , (Γ-1), equals the ratio of the escape rate to the gain rate. In this case, the escape rate representing escape downstream is $(\Gamma - 1)r_{\rm gain}(\rho)$, and for injection of N_0 particles of rigidity ρ_0 the expected differential rigidity spectrum of accelerated particles is

$$\Phi_0(\rho) = N_0(\Gamma - 1)\rho_0^{\Gamma-1}\rho^{-\Gamma}.$$

We include an extra escape term $r_{\rm esc}^{\rm max}(\rho, \rho_{\rm max})$ responsible for the "maximum rigidity" for example arising from the finite size of the accelerator (confinement limited acceleration). In the simulation with N_0 particles injected, a particle is injected at time t=0 with rigidity $\rho(0) = \rho_0$ and statistical weight $w(0) = w_0 = 1/N_0$. Its subsequent rigidity, $\rho(t)$, and weight, $w(t)$, are determined after successive time steps Δt chosen to be much smaller than the smallest time-scale in the problem. In each time step, first the rigidity is changed, $\rho(t + \Delta t) = \rho(t)[1 + \Delta t\, r_{\rm tot}(\rho)]$ where $r_{\rm tot}(\rho) = r_{\rm gain}(\rho) - r_{\rm loss,BH}(\rho)$, and then the probability of escaping in time Δt is estimated as $P_{\rm esc} = \{1 - \exp[-\Delta t\, r_{\rm esc}(\rho)]\}$. Then $w(t)P_{\rm esc}$ particles with energy E are binned in the histogram of accelerated particles for the particle's species, and the particle's weight is changed to reflect the fraction not escaping, $w(t + \Delta t) = w(t)(1 - P_{\rm esc})$. In each time step the probability of interacting is calculated, and if an interaction occurs it is simulated by Monte Carlo methods. Finally, if the time since injection exceeds a maximum time which may represent the time during which the accelerator is active, $t_{\rm active}$, the acceleration ceases and a new particle is injected. See Allard & Protheroe [16] for full details.

III. Results

We have performed simulations for different combinations of δ, $\rho_{\rm max}$ and the scaling of the IR/opt/UV, we calculated the expected output spectrum for different values of $\rho_{\rm cut}^{(p)}$ (10^{20}, 10^{21}, 10^{22} V) and various compositions injected at the shock: 100% H; 100% Fe; amixed composition (similar to low energy Galactic cosmic rays – see [3] and references therein).

Because of space limitations we include here only a subset of all our results which are presented and discussed in detail in [16], but will very briefly discuss some of the remaining cases. Fig. 2 shows the accelerated cosmic-ray spectra assuming $\rho_{\rm max} = 10^{25}$ V (which would give the same result as having an infinite shock), Kolmogorov type turbulence (e.g. diffusion coefficient rigidity-dependence index $\delta = 1/3$), a photon background equivalent to the extragalactic background, neutrons decaying inside the acceleration zone, and source activity time of 10 Gyr with the injection rate not depending on time. The spectra and compositions of nuclei accelerated are shown and normalizes such that in the absence of interactions and losses the spectra would be proportional to $\rho^{-\Gamma}$. We also show the flux of neutrinos plus antineutrinos (summed over all flavours) produced during acceleration.

For the case shown in Fig. 2, the assumed value of $\rho_{\rm max}$ is extremely high, and so the acceleration process is in this case interaction-limited for all the values of $\rho_{\rm cut}^{(p)}$ and the injected compositions we consider. In this case, there is no obvious scaling in mass or charge for the maximum reachable energy for the various species. Indeed, although the interaction threshold for a given

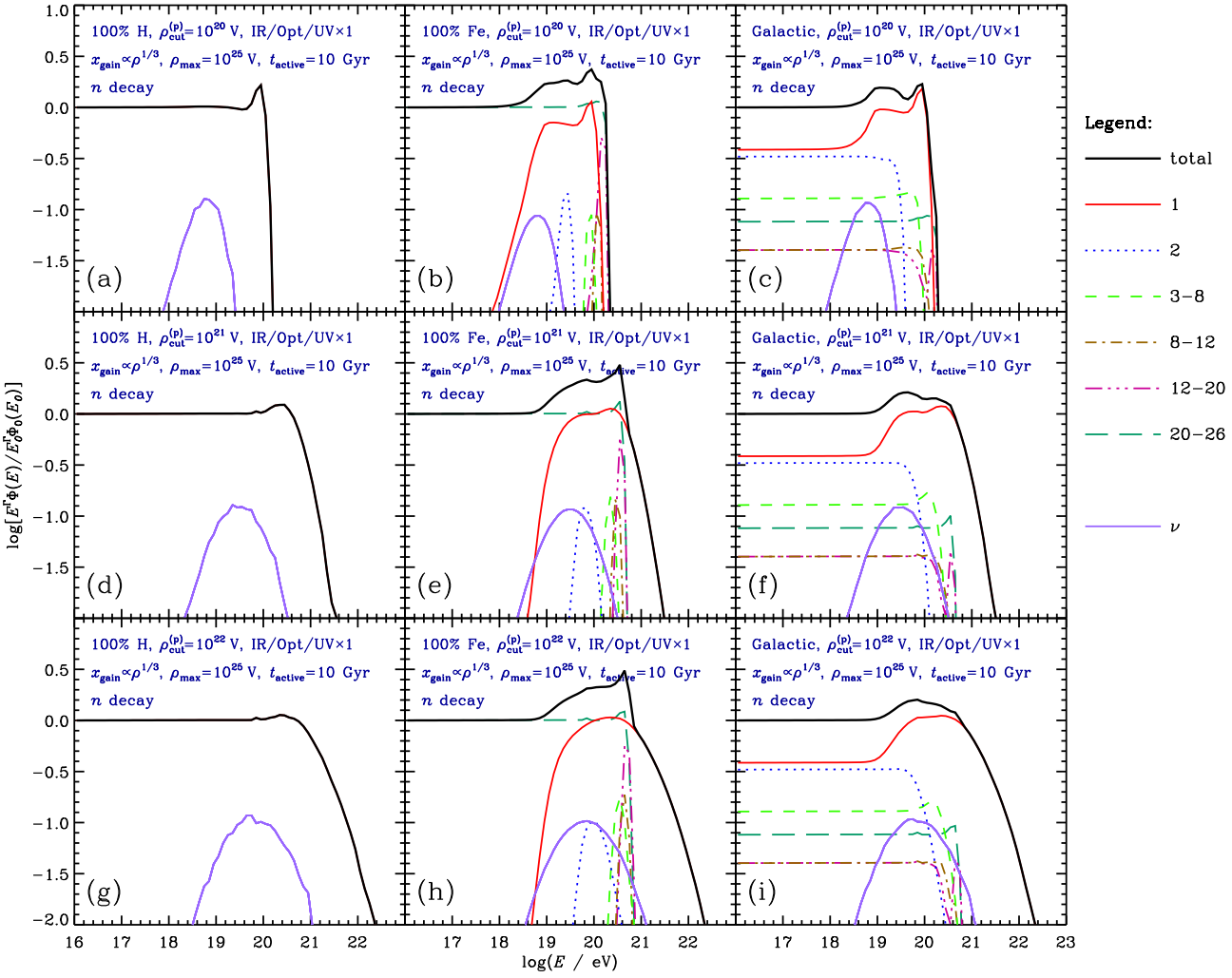

Fig. 2. Spectra of the various nuclei emerging after acceleration together with the spectra of neutrons and neutrinos (sum of all flavours) escaping from the acceleration region. The initial composition is 100% H (left column), 100% Fe (middle column), mixed composition representative of that observed in Galactic cosmic rays (right column). The acceleration rate is such that $\rho_{\rm cut}^{(p)} = 10^{20}$ V (top row), 10^{21} V (middle row), and 10^{22} V (bottom row). The IR/Opt/UV background is taken to be that at z=0, neutrons are assumed to decay inside the acceleration zone, $\kappa(\rho) \propto \rho^{1/3}$ and $\rho_{\rm max} = 10^{25}$ V. Other acceleration parameters are as indicated. Curves are for atomic numbers as indicated in the legend, with the topmost solid curve being the total spectrum, middle solid curve being Z=1, and the bottom solid curve being for the total neutrino spectrum.

photon background will occur at energies more or less proportional to the mass number of nuclei, such a scaling is not observed for the various cases studied in Fig. 2. This is because the mean free paths also scale with the mass, which means that the energy at which the photo-disintegration mean free path becomes of the same order as the acceleration length scales in a non-trivial way with mass number A. However, due to their higher interaction energy threshold and higher acceleration rate at a given energy, heavy nuclei can reach higher energies than light and intermediate nuclei.

Once the acceleration rate becomes lower than the interaction rate for a given component, a sharp cut-off takes place as the nucleus changes to a lower mass and lower energy. As can be seen in Fig. 1, the cut-off energy depends on $\rho_{\rm cut}^{(p)}$ and δ (see below). Due to the very low values of the interaction length for nuclei with CMB photons, such cut-offs seem to be extremely difficult to avoid even for very rapid acceleration (corresponding to high values of $\rho_{\rm cut}^{(p)}$). The proton component also experiences a cut-off at energies depending on $\rho_{\rm cut}^{(p)}$, this cut-off results from the increase of the loss rate due to photopion interaction. This cut-off is however smoother than in the case of nuclei due the different nature of the energy losses.

In the case we study here, i.e. acceleration not limited by confinement and a source active during the Hubble time, protons can reach an energy slightly higher than heavy nuclei, their lower acceleration rate (at a given energy) being compensated for by a lower interaction rate. In all cases, however, nuclei can reach very high energies, above 10^{20} eV for most species when the

acceleration rate is high enough ($\rho_{\rm cut}^{(p)} > 10^{21}$ eV).

One can see, in the case of a mixed composition (or in the pure iron case) that a bump of secondary protons is produced at the highest energies. The bump structure is due to the fact that the production of secondary nucleons starts quite abruptly when the acceleration rate becomes lower than the interaction rate. As a consequence, the energy at which the production of secondaries starts depends on $\rho_{\rm cut}^{(p)}$ in the same way that the cut-off energy does. After being produced, the secondary nucleons continue to be accelerated as protons (in Fig 2 we assumed neutron decay inside the box) and contribute to the proton tail at the highest energies.

IV. Conclusions

We summarize our main results shown here and elsewhere [16]. When the acceleration mechanism is not limited by confinement, protons can usually reach energies higher than nuclei which are more limited by interactions. However, this will only be the case if the ambient magnetic fields are low, as protons would then be more limited by synchrotron losses than heavy nuclei. This conclusion is particularly true for the conservative assumption that the turbulence in the vicinity of the shock is of Kolmogorov-type (i.e. a slow dependence of the acceleration rate with energy). If the turbulence brings the diffusion coefficient dependence closer to the Bohm regime (δ=1) we find that heavy nuclei can usually reach maximum energies as high as those of protons, even in the case of quite a high ambient photon field. In any case, whenever the acceleration mechanism is not confinement-limited, one cannot expect a trivial scaling of the maximum achievable energies of the various species with the mass or atomic number.

One important point to emphasize is that even when strong photon backgrounds are at play, in all cases we have considered nuclei are accelerated above 10^{19} eV whenever protons are, even though nuclei are more limited than nucleons by interactions. Hence, DSA at sources with physical conditions that would cause nuclei to be fully photodisintegrated during acceleration but allow protons to reach energies above 10^{20} eV are excluded. In other words a pure proton composition is unlikely to result from an acceleration process whenever a mixed composition is injected at a shock. A 100% proton composition would therefore require a different explanation such as injection of only protons at the shock, or propagation in a medium optically thick to photodisintegration of nuclei in the vicinity of the source.

When the acceleration becomes limited by confinement heavy nuclei are accelerated to higher energies than protons unless the acceleration is very slow and/or the photon background is very high. In the case of a maximum proton energy below 10^{20} eV, if the acceleration parameters are favorable ($\rho_{\rm cut}^{(p)} \geq 10^{21}$ eV and $\delta \sim 1$) then maximum energies proportional to atomic number are found, even in the presence of high photon backgrounds. This type of acceleration output is especially interesting in the context of recent cosmic-ray data. Indeed in the presentation of their preliminary results, the Pierre Auger Collaboration reported a composition possibly getting heavier above 10^{19} eV [17]. If this trend is confirmed, the most likely explanation would certainly involve confinement-limited acceleration with the maximum energy of the species scaling with the charge. A composition getting heavier above 10^{19} eV is indeed very difficult to obtain with propagation effects (see Allard et al., [3], [4], [5], [6]) when protons are accelerated up to the highest energies.

We have also found that nuclei should not be accelerated to energies higher than protons, in most cases, if the acceleration is interaction-limited. Interestingly, it has been shown recently (Allard et al., [6]) that the highest energy cosmic-ray spectrum can be successfully fitted by assuming a low proton maximum energy ($\sim 10^{19}$ eV) and a charge-scaling maximum energy for the other species (providing abundances of heavy nuclei slightly higher than in the Galactic cosmic rays). Although other possibilities are not ruled out, such a scenario where protons are not required to be accelerated above 10^{20} eV but where the highest energy cosmic-rays are provided by the heavy component would completely change the expectations and constraints on possible accelerators like blazars (Mücke et al. [18]) or radio-galaxies (Rachen & Biermann [19]). We shall investigate those implications in forthcoming papers. Finally, we note that confinement-limited acceleration is unlikely to provide strong neutrino fluxes at high energy.

Acknowledgments

This work was supported in part by the Australian Research Council through Discovery Project grant DP0881006 and by the Australia-France Cooperation Fund in Astronomy.

References

[1] Mücke, A. et al., 2000, Comp. Phys. Com., 124, 290
[2] Rachen, J. P. 1996, Interaction processes and statistical properties of the propagation of cosmic-rays in photon backgrounds, PhD thesis, Bonn University.
[3] Allard, D. et al., 2005, A&A, 443, L29
[4] Allard, D. et al., 2006, Journal of Cosmology and Astro-Particle Physics, 9, 5
[5] Allard, D. et al., 2007, A&A, 473, 59
[6] Allard, D. et al., 2008, Journal of Cosmology and Astro-Particle Physics, 10, 33
[7] Stecker, F. W. et al., 2006, ApJ, 648, 774
[8] Drury, L.O'C. 1983, Space Sci. Rev., 36, 57
[9] Blandford, R. & Eichler, D. 1987, Phys. Rep., 154, 1
[10] Berezhko, E.G. & Krymski, G.F. 1988, Usp. Fiz. Nauk, 154, 49
[11] Jones, F.C. & Ellison, D.C. 1991, Space Sci. Rev. 58, 259
[12] Szabo, A.P. & Protheroe, R.J. 1994, Astropart. Phys., 2, 375
[13] Protheroe, R.J. & Stanev, T. 1999, Astropart. Phys., 10, 185
[14] Drury, L.O'C. et al., 1999, A&A, 347, 370
[15] Protheroe, R.J. 2004, Astropart. Phys., 21, 415
[16] Allard, D. & Protheroe, R.J., 2009, A&A, submitted, arXiv:0902.4538
[17] Unger, M. et al. (Pierre AUGER Collaboration), 2007, Astronomische Nachrichten, 328, 614
[18] Mücke, A. et al., 2003, Astroparticle Physics, 18, 593
[19] Rachen, J.P. & Biermann, P.L. 1993, A&A, 272, 161